

Runaway Massive Binaries and Cluster Ejection Scenarios

M. Virginia McSwain¹

Department of Astronomy, Yale University, P.O. Box 208101, New Haven, CT 06520-8101
 mcswain@astro.yale.edu

Scott M. Ransom

National Radio Astronomy Observatory, 520 Edgemont Road, Charlottesville, VA 22903
 sransom@nrao.edu

Tabetha S. Boyajian, Erika D. Grundstrom

Department of Physics and Astronomy, Georgia State University, P.O. Box 4106, Atlanta, GA 30302-4106
 tabetha@chara.gsu.edu, erika@chara.gsu.edu

Mallory S. E. Roberts

Eureka Scientific, Inc., 2452 Delmer Street Suite 100, Oakland, CA 94602-3017
 malloryr@gmail.com

ABSTRACT

The production of runaway massive binaries offers key insights into the evolution of close binary stars and open clusters. The stars HD 14633 and HD 15137 are rare examples of such runaway systems, and in this work we investigate the mechanism by which they were ejected from their parent open cluster, NGC 654. We discuss observational characteristics that can be used to distinguish supernova ejected systems from those ejected by dynamical interactions, and we present the results of a new radio pulsar search of these systems as well as estimates of their predicted X-ray flux assuming that each binary contains a compact object. Since neither pulsars nor X-ray emission are observed in these systems, we cannot conclude that these binaries contain compact companions. We also consider whether they may have been ejected by dynamical interactions in the dense environment where they formed, and our simulations of four-body interactions suggest that a dynamical origin is possible but unlikely. We recommend further X-ray observations that will conclusively identify whether HD 14633 or HD 15137 contain neutron stars.

Subject headings: binaries: spectroscopic, stars: early-type, stars: kinematics, stars: winds, stars: individual (HD 14633, HD 15137), open clusters and associations: individual (NGC 654), pulsars: general, X-rays: binaries

1. Introduction

While most O- and B-type stars are believed to form in open clusters and stellar associations,

some are observed at high galactic latitudes and with large peculiar space velocities. The estimated fraction of O stars that are runaways ranges from 7% (Conti, Leep, & Lorre 1977) to 49% (Stone 1979). These stars were likely ejected from the clusters of their birth, and there are two accepted

¹NSF Astronomy and Astrophysics Postdoctoral Fellow

mechanisms to explain the origin of their runaway velocities. Close multi-body interactions in a dense cluster environment may cause one or more stars to be scattered out of the region (Poveda, Ruiz, & Allen 1967). On the other hand, a supernova explosion within a close binary may eject the secondary star due to the conservation of momentum of mass lost in the explosion, including supernova kicks (Zwicky 1957; Blaauw 1961; Sutantyo 1978).

The production of runaway O- and B-type binaries is expected to be rare, but these systems can offer key insights into the evolution of close binary stars and open clusters. Distinguishing between the dynamical ejection and binary supernova scenarios for an isolated runaway star can be nearly impossible unless the star contains CNO-processed gas received from a past episode of mass transfer (Hoogerwerf, de Bruijne, & de Zeeuw 2001). However, the ejection mechanism responsible for producing runaway binaries can be distinguished more easily from a variety of observable properties.

Leonard & Duncan (1990) use N -body simulations of open clusters to show that a binary frequency of about 10% is expected from dynamical ejections. Most of their simulated binaries have eccentric orbits, $0.4 < e < 0.7$, and high mass ratios, $q = M_2/M_1 > 0.5$. While Leonard & Duncan (1990) do not discuss the resulting orbital periods in their simulations, we do not expect long period ($P > 1000$ days) binaries to form via dynamical interactions since their low binding energies would likely cause them to be ionized. On the other hand, Portegies Zwart (2000) predicts a higher binary fraction of 20–40% among runaways which are ejected by supernovae in close binaries. The resulting neutron star may remain bound to the secondary if not enough mass is lost during the explosion or if the explosion is not symmetric (producing a kick velocity). In such cases, the present-day orbital period and eccentricity depend on the mass ejected during the supernova and the kick velocity (Nelemans, Tauris, & van den Heuvel 1999; Brandt & Podsiadlowski 1995), but the resulting period distribution is expected to be 3–1000 days (Portegies Zwart 2000).

Distinguishing between the dynamical or supernova ejection mechanisms among runaway spectroscopic binaries can be a difficult task since

both are expected to produce eccentric, relatively short period binaries. Only dynamical interactions are expected to produce double-lined spectroscopic binaries (SB2s), while a single-lined system (SB1) may be formed either way. Obtaining very high signal-to-noise (S/N) spectra or performing doppler tomography can, in some cases, identify optical companions in such systems. However, it can be nearly impossible to detect a cool, low mass, optical companion with an O- or B-type primary.

Neutron star companions can be difficult to identify as well. A few runaway O stars are predicted to be associated with pulsars (Portegies Zwart 2000), but so far none have been found (Philp et al. 1996; Sayer, Nice, & Kaspi 1996). X-ray emission may also be used to pinpoint neutron star companions since a neutron star may accrete mass from its companion via a Roche lobe overflow stream or by Bondi-Hoyle accretion from the stellar wind of the luminous primary (Bondi & Hoyle 1944; Davidson & Ostriker 1973; Kaper 1998). The systems experiencing Roche lobe overflow usually have large X-ray luminosities and striking optical emission lines. On the other hand, weaker X-ray emission will result if stellar winds are the accretion source. According to the wind accretion model, the observed X-ray luminosity depends on the system separation, the relative wind and companion velocities, the stellar mass-loss rate, and the mass of the accretor (Lamers, van den Heuvel, & Petterson 1976). If the stellar wind is too weak, or the system separation too large, the X-ray luminosity would diminish below the detection limit of today’s X-ray surveys, hence a “quiet” massive X-ray binary (MXRB).

We have recently completed a radial velocity study of 12 field and runaway O- and B-type stars to identify spectroscopic binaries with high space velocities (McSwain et al. 2007). In that work, we improved the orbital elements of five SB1s, but among these only two are definitely runaways: HD 14633 and HD 15137. HD 14633 is classified as an ON8.5 V star, and HD 15137 is somewhat more evolved as an O9.5 III(n) star. Boyajian et al. (2005) found that these runaway SB1 systems were likely ejected in separate events from the open cluster NGC 654, but the travel times since their ejection (14 Myr for HD 14633 and 10 Myr for

HD 15137) present an unusual paradox since they are longer than the expected lifetimes of O-type stars. They attempted doppler tomographic separation for both systems, but this search for an optical companion was unsuccessful. HD 14633 is a nitrogen-strong star (Walborn 1972), and Boyajian et al. argue that its nitrogen enrichment and fast rotation resulted from a mass transfer episode prior to a supernova in the close binary system. They propose that both stars are quiet MXRB candidates that harbor neutron star companions but are not known X-ray emitters.

To investigate this claim, we present here the results of a pulsar search in these two systems. We also compare the observed upper limits of their X-ray fluxes to model predictions of X-rays generated by the accretion of stellar winds onto a compact companion. Since neither pulsars nor X-ray emission are detected, we are not certain that either system contains the product of a supernova. Therefore we also investigate the possibility that dynamical interactions may have been responsible for their ejection from NGC 654.

2. Constraints on the Secondary Masses

We recently presented updated orbital elements and mass functions, $f(m)$, for the SB1 systems HD 14633 and HD 15137 (McSwain et al. 2007), and these parameters are summarized in Table 1. While $f(m)$ does not strictly define the component masses, it does allow constraints on the primary star’s mass, M_1 , the companion mass, M_2 , and the system inclination, i . We plot the relationships between these properties in Figures 1 and 2 using a grid of values for M_1 . In addition, the vertical dashed line in both figures indicates the expected mass of each star based on the calibration of Martins, Schaerer, & Hillier (2005). Both binaries have very low $f(m)$ that suggest low mass companions ($1-3M_\odot$). Without directly detecting the companions, we must constrain their masses using another method.

We used the statistical method of Mazeh & Goldberg (1992) to determine the most probable q , and this relationship is plotted as a solid line in the top panels of Figures 1 and 2. Note that their technique results in a somewhat lower probable value for i than the expectation value $\langle i \rangle \sim 60^\circ$ since it accounts for observational selection effects. HD

14633 and HD 15137 are particularly interesting since they probably have $q < 0.3$, and such low q are unknown among O star binaries (excluding X-ray binaries). Their allowed masses do not exclude neutron star companions, and below we investigate the possibility of radio pulsars or a detectable X-ray signature of a compact companion.

3. Pulsar Search Results

HD 14633 was targeted in a previous search for pulsars in runaway OB stars by Philp et al. (1996). Although they did not find any pulsars, we chose to perform a new, more sensitive search to investigate the companions of both runaway binaries. Portegies Zwart (2000) shows that detection of pulsars in O star binaries is hindered by the absorption of the radio emission by the stellar winds. This absorption will be greater at periastron than apastron since the winds are densest close to the O star, and our new ephemerides for these binaries (McSwain et al. 2007) allowed us to schedule the observations as close as possible to the maximum separation. (If these systems have high i , true if a neutron star is present, the times of inferior conjunctions may provide the lowest column depth instead. These times correspond to the orbital phases 0.83 for HD 14633 and 0.70 for HD 15137. Although our observations were not timed to occur at inferior conjunction, they are well separated from superior conjunction when the neutron star could possibly be eclipsed.) We also chose to use higher frequencies than the previous investigations because they are more likely to detect radio pulses dispersed by the stellar winds.

We observed HD 14633 and HD 15137 using the National Radio Astronomy Observatory’s 100-m Green Bank Telescope (GBT) and the Pulsar Spigot back-end (Kaplan et al. 2005). We used the Spigot in mode 2 with the S-band receiver to obtain 600 MHz (1650-2250 MHz) of bandwidth, which the Spigot summed and synthesized into 768 0.78125-MHz frequency channels every 81.92 μ s. The Spigot in mode 42, with the 820 MHz receiver, provided 50 MHz of bandwidth (795-845 MHz), summed into 1024 0.0488-MHz frequency channels with the same time resolution. Each target was observed once with each receiver for 6300 s. For each observation, the time at midexposure and the corresponding orbital phase are listed in

Table 2. Although we requested observations at the times of apastron (orbital phase 0.5), telescope scheduling constraints limited us to slightly earlier times during each orbit.

The data were reduced using the PRESTO software package (Ransom 2001). We first searched the raw data for radio frequency interference in both the time and frequency domains and applied interference masks to remove these sources. Each of our targets is expected to have a dispersion measure (DM) $\sim 50 - 75 \text{ pc cm}^{-3}$ using the NE2001 model (Cordes & Lazio 2002) with the distances in Table 1 (McSwain et al. 2007), so we searched the observations by dedispersing the raw data into separate time series with DMs ranging from 0 to 120 pc cm^{-3} and spaced by 0.5 pc cm^{-3} . We then Fourier-transformed each time series and searched them by using Fourier-domain acceleration search techniques in order to maintain sensitivity to both pulsars in binary orbits as well as isolated pulsars. For the acceleration search, this technique involves a linear approximation of the binary’s orbital acceleration (valid since the observations span a small fraction of the orbit) to look for a derivative in pulsar frequency. The flux density sensitivity, S_{lim} , and luminosity, L_{lim} , limits of each observation are listed in Table 2. The typical pulsar has a luminosity $L \gtrsim 0.1 \text{ mJy kpc}^2$ at 1400 MHz (Lorimer et al. 2006), and our L_{lim} do go fainter than this value for the S-band observations.

While we did not detect any pulsars in these systems, we cannot rule out their existence since a pulsar’s beam may not cross our line of sight. Tauris & Manchester (1998) find that the observed beaming fraction depends on the rotational period, P , since the beam radius varies as $P^{-1/2}$. P , in turn, depends on the pulsar’s age, t , since magnetic dipole radiation causes the pulsar to spin down over time. Without detecting a pulsar we cannot measure P directly, but if the runaways were ejected by supernovae, their dynamical ages correspond to the ages of the resulting neutron star. HD 14633 was ejected from the open cluster NGC 654 about 14 Myr ago, and HD 15137 left the same cluster about 10 Myr ago (Boyajian et al. 2005). If we assume that any pulsar was born spinning much faster than its current rate, we can

use

$$P \approx \sqrt{\frac{8\pi^2 R^6}{3c^3 I}} B^2 t, \quad (1)$$

where R is the neutron star radius, c is the speed of light, I is the moment of inertia, B is the strength of the magnetic field, and t is the pulsar age in seconds (Tauris & Manchester 1998). Using typical neutron star values of $R = 10 \text{ km}$, $I = 10^{45} \text{ g cm}^2$, and $B = 10^{12} \text{ G}$ (Lipunov 1992), we estimate $P \approx 1 \text{ s}$ for HD 14633 and HD 15137. Lorimer et al. (2006) find a beaming fraction of $\sim 20\%$ for such pulsars, making it unlikely that we will detect the beam.

Clearly, our GBT observations are not sufficient to characterize the companions in either system. Below we investigate their other properties to determine if they should display an observable X-ray luminosity.

4. Predicted X-ray Luminosities

4.1. Wind Accretion Model

HD 14633 and HD 15137 are SB1s with high eccentricity, but neither are known X-ray sources. If they do contain compact companions, should these stars have a detectable X-ray emission? We predict the X-ray flux of each quiet MXRB candidate using the wind accretion model of Lamers et al. (1976), modified for eccentric orbits. This method uses the Bondi-Hoyle accretion rate

$$S_a = \frac{\pi R_a^2 \dot{M}}{4\pi a^2} \quad (2)$$

(Lamers et al. 1976), which depends on the stellar mass loss rate, \dot{M} , the system’s major axis, a , and the accretion radius of the companion,

$$R_a = \frac{2GM_2}{V_{rel}^2}. \quad (3)$$

Here, M_2 is the mass of the accretor and V_{rel} is the relative velocity of the stellar wind and the companion’s orbit, V_{wind} and V_{orb} respectively. V_{orb} is determined from a and the orbital eccentricity, e . The predicted X-ray luminosity is

$$L_X \propto \zeta S_a M_2 \quad (4)$$

(Lamers et al. 1976). The efficiency, ζ , of converting accreting matter into X-ray luminosity is approximately 0.1 for neutron stars and black holes

(Lamers et al. 1976). The observed X-ray flux will also depend on the system distance, d , and the H I column density, $n\text{H}$. While the Lamers et al. model is useful for estimating the integrated X-ray flux produced by wind accretion, we emphasize that it is an approximation that does not include any spectral information about the emission. Therefore the predicted X-ray emission should be viewed with some caution.

We could not measure the mass loss rate, \dot{M} , from our optical spectra (McSwain et al. 2007) since we did not observe the $\text{H}\alpha$ line. Instead we obtained published values of the observed \dot{M} for each star. Chlebowski & Garmany (1991) and Howarth & Prinja (1989) found values for HD 14633 of $\log \dot{M} = -6.81 M_{\odot} \text{ yr}^{-1}$ and $-6.9 M_{\odot} \text{ yr}^{-1}$, respectively. We adopt the lower value for our model of the wind accretion. Howarth & Prinja (1989) also measured $\log \dot{M} = -6.5 M_{\odot} \text{ yr}^{-1}$ for HD 15137.

We measured their terminal wind velocities, V_{∞} , using flux-calibrated UV spectra obtained from the *International Ultraviolet Explorer (IUE)* archives. Prinja, Barlow, & Howarth (1990) describe how to use either the time-variable narrow absorption components of UV lines or the more steady-state, saturated line edge to measure V_{∞} , and we chose this latter technique due to the low S/N of the *IUE* spectra. For HD 14633, we co-added the available high dispersion, Short Wavelength Prime Camera (SWP) spectra and looked for saturation in the N V $\lambda 1238.821$, Si IV $\lambda 1393.76$, and C IV $\lambda 1548.202$ lines. V_{∞} corresponds to the blue edge of the saturated line profile. HD 15137 has only one high dispersion SWP spectrum available, so we binned this by 5 pixels to improve the S/N, reducing the precision of our measurement. The resulting values of V_{∞} are listed in Table 3, and they agree well with the values found by Howarth et al. (1997). Knowledge of V_{∞} enables us to characterize the stellar wind in the vicinity of the star according to the wind velocity law

$$V(r) = V_{\infty} \left(1 - \frac{R_{\star}}{r} \right)^{\beta} \quad (5)$$

with $\beta = 0.8$ for weak stellar winds (Howarth & Prinja 1989; Puls et al. 1996).

The remaining input parameters for the wind accretion model come from our orbital solutions,

SED fits, and stellar distances (McSwain et al. 2007). We used a grid of values for M_1 with the minimum M_2 allowed by the mass functions ($i = 90^{\circ}$). For these eccentric binary orbits, we expect the accretion rate to be greatest just after periastron, where the wind density is higher and its velocity slower relative to the companion. Therefore we calculated the time-averaged X-ray flux, F_X , as well as the expected maximum and minimum flux during the orbit as a function of the primary mass. The results are illustrated in the bottom panels of Figures 1 and 2. We note that a higher M_2 increases the predicted X-ray flux since the gravitational force accreting the wind is larger.

Normal O stars are expected to have an intrinsic X-ray flux due to shocks in their stellar winds (Sana et al. 2006 and references therein). The winds are driven by the absorption and reemission of UV photons in the spectral lines, and small-scale instabilities in the wind will quickly grow into shocks (Lamers & Cassinelli 1999). Magnetic confinement of the stellar winds and colliding winds in close, massive binaries may also contribute to the X-ray emission (Sana et al. 2006 and references therein). Sana et al. (2006) found that, with the exception of two colliding wind binaries, all of the binary and single O-type stars in the open cluster NGC 6231 display a tight correlation between their bolometric luminosities, L_{bol} , and their X-ray luminosities, L_X , in the 0.5 – 10.0 keV band. Thus the intrinsic X-ray emission of an O star can be predicted from the relation,

$$\log L_X - \log L_{bol} = -6.912 \pm 0.153 \quad (6)$$

(Sana et al. 2006). Using L_{bol} from the calibration of Martins et al. (2005), we find that HD 14633 and HD 15137 each have an intrinsic L_X of 2×10^{31} to $3 \times 10^{31} \text{ erg s}^{-1}$. With the adopted distances given in Table 1 (McSwain et al. 2007), this corresponds to an unabsorbed flux between 3×10^{-14} and $7 \times 10^{-14} \text{ erg cm}^{-2} \text{ s}^{-1}$, a negligible contribution to the predicted flux from stellar wind accretion.

4.2. Observed Upper Limits

Since these stars have not been detected as X-ray sources, we estimate an upper limit for their unabsorbed X-ray fluxes using other detected sources from the *ROSAT* All-Sky Survey and pointed *ROSAT* observations within a 30' radius

of each star (White, Giommi, & Angelini 2000; Voges et al. 2000). We expect that wind accretion will generate X-rays having a power law spectrum typical of MXRBs, and we used the photon index $\Gamma = 2.0$ from the microquasar LS 5039 (another wind-accreting MXRB; Bosch-Ramon et al. 2005). MXRBs in a low/hard emission state generally have $\Gamma \sim 1.6$ (Belloni 2001), which we also consider. The Galactic H I column density, nH , for each target was calculated using NASA’s HEASARC tool¹. Finally, we used the HEASARC WebPIMMS calculator² to convert the upper limit of the X-ray count rate to the expected unabsorbed flux in the 0.5–10 keV range. These details and the resulting upper limits for F_X are listed in Table 4. We compare these upper limits to the predicted F_X in the bottom panels of Figures 1 and 2. In each case, the observed upper limit is higher than the intrinsic X-ray flux from the O-star, consistent with the non-detection of each star.

The wind accretion model predicts X-ray fluxes of HD 14633 and HD 15137 that are at least an order of magnitude greater than the observed upper limits for the most likely O star masses. However, it is worth noting that the wind-accreting microquasar LS 5039 exhibits order-of-magnitude variations in both its X-ray flux and mass-loss rates (Bosch-Ramon et al. 2005; McSwain et al. 2004), and other MXRBs may have flux variations of order 100 (Belloni 2001). If the *ROSAT* observations occurred during times of low stellar mass loss, it is possible that any X-ray emission from a neutron star might be below the detection limit. O star winds may also attenuate any X-ray emission in low energy bands, and Sana et al. (2004) find order-of-magnitude variations in the X-ray emission from the colliding wind binary HD 152248 due to variations in the absorption with orbital motion. If HD 14633 and HD 15137 are high inclination systems, they may experience similar variations.

4.3. Quiescent Neutron Stars

Could these binaries contain neutron stars in a quiescent state? The conditions for wind ac-

¹The HEASARC nH calculator is available online at <http://heasarc.nasa.gov/cgi-bin/Tools/w3nh/w3nh.pl>.

²The WebPIMMS calculator is available online at <http://heasarc.nasa.gov/Tools/w3pimms.html>.

cretion onto a neutron star depend strongly upon the spin rate and the magnetic field, and these are discussed in detail by Lipunov (1992). A young neutron star will not accrete significant amounts of material because its fast rotation and large magnetic field sweep material out of the system at a distance larger than the accretion capture radius, R_a . Systems in this ejector regime are often observed as pulsars, and they are expected to remain in this state for $10^5 - 10^6$ years. The spinning magnetic field will dissipate rotational energy, causing the neutron star to spin down with time. The neutron star passes into the propellor regime, where the magnetospheric radius, R_{mag} , is smaller than R_a but remains larger than the corotation radius, R_c . The rapid rotation continues to inhibit accretion onto the neutron star. Eventually the compact star spins down enough to allow R_c to expand outward beyond R_{mag} , trapping material in the vicinity of the neutron star and allowing accretion to begin.

We can investigate whether the proposed neutron stars should be in the accretion regime using these characteristic distances given by Lipunov (1992). Assuming a nominal $M_2 = 1.4 M_\odot$ for the neutron star and using the relative wind/orbital velocity $V_{rel} \sim 1500 \text{ km s}^{-1}$ for both systems, their accretion capture radius is

$$R_a = \frac{2GM_2}{V_{rel}^2} \sim 2 * 10^{10} \text{ cm.} \quad (7)$$

Using the rotational frequency $\omega \approx 1 \text{ s}^{-1}$ (discussed in Section 3), we can estimate the corotation radius as

$$R_c = \left(\frac{GM_2}{\omega^2} \right)^{1/3} \sim 6 * 10^8 \text{ cm.} \quad (8)$$

The magnetospheric radius, R_{mag} , can be determined by equating the ram pressure of the accreting gas to the magnetic field pressure. While we cannot measure the magnetic moment, μ , the observed range among other neutron stars is 10^{28} to $10^{31.5} \text{ G cm}^3$, with the most typical value being 10^{30} G cm^3 (Lipunov 1992). Thus we find

$$R_{mag} = \left(\frac{\mu^2}{2S_a \sqrt{2GM_2}} \right)^{2/7} \sim 3 * 10^9 \text{ cm} \quad (9)$$

for both binaries. Unrestrained accretion onto the neutron star requires that $R_{mag} < R_a$ and $R_{mag} <$

R_c , which may be possible in these systems given the large uncertainties in R_c and R_{mag} .

HD 14633 and HD 15137 could contain neutron stars in a low accretion state, and new X-ray observations should conclusively show whether these systems harbor compact companions. Even quiescent neutron stars are expected to produce an X-ray luminosity of 10^{30} to 10^{34} erg s $^{-1}$ with a thermal or nonthermal spectrum (Lipunov 1992), somewhat comparable in magnitude to the expected intrinsic luminosity of an O star but presumably distinguishable by the spectral energy distribution. Therefore any detection of X-rays with some spectral resolution should be able to distinguish between the soft spectrum of stellar wind emission, the presence of a quiescent neutron star, or emission produced by wind accretion with a power law spectrum.

5. The Dynamical Interaction Scenario

Both HD 14633 and HD 15137 contain a secondary star with a minimum mass $M_2 = 1 - 2 M_\odot$, so a neutron star companion seems plausible. However, we do not detect pulsars in either system, and neither HD 14633 nor HD 15137 exhibits evidence of X-rays produced by accretion onto a compact companion. Although we have discussed several reasons to account for the lack of radio or X-ray detections, we must explore the possibility that neutron stars are not present in these systems. We consider here whether these runaway SB1s may have been ejected from NGC 654 by close dynamical encounters in the open cluster.

In our earlier study of these runaway stars (Boyajian et al. 2005), we thought the dynamical interaction scenario unlikely based on the low mass ratios, $q < 0.3$, of HD 14633 and HD 15137. There are no known O stars in close, spectroscopic binaries that contain main sequence or pre-main sequence companions later than mid B-type stars (Pourbaix et al. 2004), and binary O-type stars usually form in open clusters with $q \sim 1$ (Clarke & Pringle 1992 and references therein). Therefore it is unlikely that these binaries were born with low q and then ejected. However, the current mass ratios can be explained by dynamical interaction scenarios that exchange binary partners (e.g. Gualandris, Portegies Zwart, & Eggleton 2004).

The pairs may have formed in separate exchanges involving a wide O-type pair and a close B-type pair with a comparable binding energy. Such interactions can also explain the high e of the resulting binaries. They would retain this eccentricity for more than 10^{10} years since the low mass ratio significantly increases the timescale of tidal circularization of the orbit (Hilditch 2001).

To test the plausibility of this dynamical origin, we simulated the ionization of a wide O-type binary in three- and four-body scattering interactions using the Starlab package developed by P. Hut, S. McMillan, J. Makino, and S. Portegies Zwart. In each simulation, we assumed a $20 M_\odot + 20 M_\odot$ pair in a circular orbit with a semi-major axis of 1 AU. The radius of each O star was set to $8 R_\odot$ to represent a typical unevolved pair of late O-type stars. In our three-body simulations, we used a projectile consisting of a single $5 M_\odot$ star with radius $4 R_\odot$ and velocity of 140 km s^{-1} . The B-type projectile with this velocity at infinity would approach the O star binary with a kinetic energy, K , of only 0.13 times the gravitational potential energy of the binary, making an ionization extremely unlikely. In 50,000 three-body simulations in which we allowed the impact parameter of the projectile, r , to vary from 0 to 5 AU, the target binary became unbound in fewer than 1% of our trials. For $r > 1.25$ AU, the chance of ionization decreased to nearly zero. Increasing K by factors of 2 and 3 (to achieve incoming velocities of 200 km s^{-1} and 240 km s^{-1} , respectively) reduced the number of ionizations further.

A four-body interaction is far more likely to separate an O star binary. For these simulations, we used a target pair identical to that described above, and the projectile consisted of a $5 M_\odot + 5 M_\odot$ pair of B-type stars in a circular orbit with a semi-major axis of 0.12 AU. We performed 8200 simulations using the same range in K as above, thereby allowing incoming velocities of $100 - 170 \text{ km s}^{-1}$ for the projectile binary, and allowing r to vary from 0 to 5 AU. The O binary was ionized in 11% of our trials. We observe no strong dependence on the ionization rate for $r < 5$ AU with the lowest K , although higher K projectiles produce fewer ionizations when $r > 3$ AU (they tend to fly past the target binary, preserving the original configurations).

In most of our four-body trials, Starlab pre-

dicted collisions between the targets and/or projectiles, regardless of whether the target binary became separated. Without a robust hydrodynamical simulation, it is difficult to accurately predict how many four-body interactions would result in a close, bound pair in a binary-binary exchange rather than a stellar collision. Nevertheless, our simulations did predict a small number of exchanges (10) in the four-body scattering scenario.

6. Conclusions

Certainly it is plausible that HD 14633 and HD 15137 were both ejected in multi-body encounters in the dense open cluster NGC 654. Simulations of a typical four-body interaction suggest that 11% of encounters between low mass ($5 M_{\odot} + 5 M_{\odot}$) binaries will ionize an O star pair ($20 M_{\odot} + 20 M_{\odot}$). However, this rate is too low for such a dynamical interaction to be probable, and we cannot conclude that these binaries were ejected from NGC 654 through such an interaction.

While we do not presently detect a neutron star in either system, we cannot rule out that these systems were ejected by supernovae in the close binary systems. We recommend performing further X-ray observations deep enough to detect the intrinsic emission from the stellar wind shocks in these O stars. Any additional emission from a quiescent neutron star or from active accretion onto its surface should be comparable to or stronger than the intrinsic wind emission, thereby producing a measurable X-ray excess. Such observations are necessary to determine whether these systems contain neutron stars and thus determine conclusively which mechanism is responsible for producing these runaway binary systems.

We thank Charles Bailyn, Doug Gies, and the referee, Simon Portegies Zwart, for their helpful discussions about this work. The GBT observations would not be possible without their friendly and diligent staff, especially David Rose, Becky Warner, and Shirley Curry. M. V. M. gratefully acknowledges travel support from NRAO, and she is supported by an NSF Astronomy and Astrophysics Postdoctoral Fellowship under award AST-0401460. This material is based on work supported by the National Science Foundation under

Grants No. AST-0205297 and AST-0506573 (D. R. G.). Institutional support has been provided from the GSU College of Arts and Sciences and from the Research Program Enhancement fund of the Board of Regents of the University System of Georgia, administered through the GSU Office of the Vice President for Research. The National Radio Astronomy Observatory is a facility of the National Science Foundation operated under cooperative agreement by Associated Universities, Incorporated. Some of the data presented in this paper were obtained from the Multimission Archive at the Space Telescope Science Institute (MAST). STScI is operated by the Association of Universities for Research in Astronomy, Inc., under NASA contract NAS5-26555. Support for MAST for non-HST data is provided by the NASA Office of Space Science via grant NAG5-7584 and by other grants and contracts. This research has made use of data obtained from the High Energy Astrophysics Science Archive Research Center (HEASARC), provided by NASA's Goddard Space Flight Center.

Facilities: GBT, IUE(SWP), ROSAT(PSPC)

REFERENCES

- Belloni, T. 2001, astro-ph/0112217
- Blaauw, A. 1961, *Bull. Astron. Inst. Netherlands*, 15, 26
- Bondi, H., & Hoyle, F. 1944, *MNRAS*, 104, 273
- Bosch-Ramon, V., Paredes, J. M., Ribó, M., Miller, J. M., Reig, P., & Martí, J. 2005, *ApJ*, 628, 388
- Boyajian, T. S., Beaulieu, T. D., Gies, D. R., Huang, W., McSwain, M. V., Riddle, R. L., Wingert, D. W., & De Becker, M. 2005, *ApJ*, 621, 978
- Brandt, N., & Podsiadlowski, P. 1995, *MNRAS*, 274, 461
- Chlebowski, T., & Garmany, C. D. 1991, *ApJ*, 368, 241
- Clarke, C. J., & Pringle, J. E. 1992, *MNRAS*, 255, 423
- Conti, P. S., Leep, E. M., & Lorre, J. J. 1977, *ApJ*, 214, 759

- Cordes, J. M., & Lazio, T. J. W. 2002, *astro-ph/0207156*
- Davidson, K., & Ostriker, J. P. 1973, *ApJ*, 179, 585
- Gualandris, A., Portegies Zwart, S., & Eggleton, P. P. 2004, *MNRAS*, 350, 615
- Hilditch, R. W. 2001, *An Introduction to Close Binary Stars* (Cambridge: Cambridge Univ. Press)
- Hoogerwerf, R., de Bruijne, J. H. J., & de Zeeuw, P. T. 2001, *A&A*, 365, 49
- Howarth, I. D., Siebert, K. W., Hussain, G. A. J., & Prinja, R. K. 1997, *MNRAS*, 284, 265
- Howarth, I. D., & Prinja, R. K. 1989, *ApJS*, 69, 527
- Kaper, L. 1998, in *ASP Conf. Ser. 131, Boulder-Munich II: Properties of Hot, Luminous Stars*, ed. I. D. Howarth (San Francisco: ASP), 427
- Kaplan, D. L., et al. 2005, *PASP*, 117, 643
- Lamers, H. J. G. L. M., & Cassinelli, J. P. 1999, *Introduction to Stellar Winds* (Cambridge: Cambridge Univ. Press)
- Lamers, H. J. G. L. M., van den Heuvel, E. P. J., & Petterson, J. A. 1976, *A&A*, 49, 327
- Leonard, P. J. T., & Duncan, M. J. 1990, *AJ*, 99, 608
- Lipunov, V. M. 1992, *Astrophysics of Neutron Stars* (Berlin: Springer-Verlag)
- Lorimer, D. R., et al. 2006, *MNRAS*, 372, 777
- Martins, F., Schaerer, D., & Hillier, D. J. 2005, *A&A*, 436, 1049
- Mazeh, T., & Goldberg, D. 1992, *ApJ*, 394, 592
- McSwain, M. V., Boyajian, T., Grundstrom, E., & Gies, D. R. 2007, *ApJ*, 655, in press (January 20, 2007 issue; *astro-ph/0608270*)
- McSwain, M. V., Gies, D. R., Huang, W., Wiita, P. J., Wingert, D. W., & Kaper, L. 2004, *ApJ*, 600, 927
- Nelemans, G., Tauris, T. M., & van den Heuvel, E. P. J. 1999, *A&A*, 352, 87
- Pandey, A. K., Upadhyay, K., Ogura, K., Sagar, R., Mohan, V., Mito, H., Bhatt, H. C., & Bhatt, B. C. 2005, *MNRAS*, 358, 1290
- Philp, C. J., Evans, C. R., Leonard, P. J. T., & Frail, D. A. 1996, *AJ*, 111, 1220
- Portegies Zwart, S. F. 2000, *ApJ*, 544, 437
- Pourbaix, D., Tokovinin, A. A., Batten, A. H., Fekel, F. C., Hartkopf, W. I., Levato, H., Morrell, N. I., Torres, G., & Udry, S. 2004, *A&A*, 424, 727
- Poveda, A., Ruiz, J., & Allen, C. 1967, *Bol. Obs. Tonantzintla Tacubaya*, 4, 86
- Prinja, R. K., Barlow, M. J., & Howarth, I. D. 1990, *ApJ*, 361, 607
- Puls, J., et al. 1996, *A&A*, 305, 171
- Ransom, S. M. 2001, Ph.D. thesis, Harvard University
- Sana, H., Rauw, G., Nazé, Y., Gosset, E., & Vreux, J.-M. 2006, *MNRAS*, 372, 661
- Sana, H., Stevens, I. R., Gosset, E., Rauw, G., & Vreux, J.-M. 2004, *MNRAS*, 350, 809
- Sayer, R. W., Nice, D. J., & Kaspi, V. M. 1996, *ApJ*, 461, 357
- Stone, R. C. 1979, *ApJ*, 232, 520
- Sutantyo, W. 1978, *Ap&SS*, 54, 479
- Tauris, T. M., & Manchester, R. N. 1998, *MNRAS*, 298, 625
- Urban, S. E., Zacharias, N., & Wycoff, G. L. 2004, U. S. Naval Observatory, Washington, D. C. (VizieR No. I/294)
- Voges, W., et al. 2000, *IAU Circ.*, 7432, 1
- Walborn, N. R. 1972, *AJ*, 77, 312
- White N. E., Giommi P., & Angelini L. 2000, The WGACAT version of the ROSAT PSPC Catalogue, Rev. 1, VizieR IX/31
- Zwicky, F. 1957, *Morphological Astronomy* (Berlin: Springer)

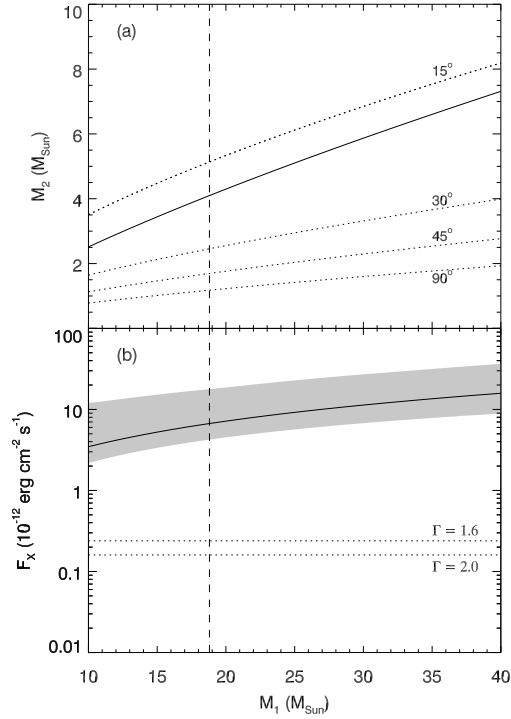


Fig. 1.— (a) The mass diagram of HD 14633 is plotted for a range of inclination angles (*dotted lines*). The most probable values of M_2 from Mazeh & Goldberg (1992) (*solid line*) and the expected M_1 from Martins et al. (2005) (*vertical dashed line*) are also shown. (b) Predicted time-averaged X-ray flux (*solid line*) and the predicted range in flux over the eccentric orbit (*gray*) are shown for the lowest possible M_2 . The observed upper limits for F_X are shown for comparison (*dotted lines*).

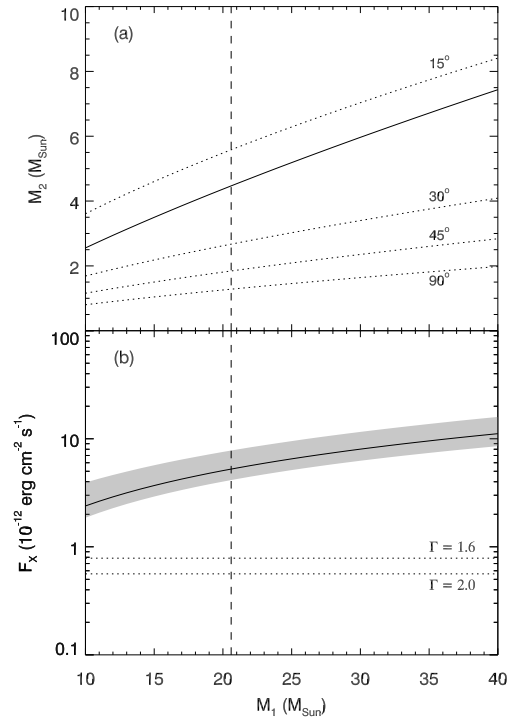


Fig. 2.— The mass diagram and predicted X-ray flux are plotted for HD 15137 in the same format as Figure 1.

TABLE 1
SUMMARY OF RESULTS FROM MCSWAIN ET AL. 2007

| Star | P (d) | e | $f(m)$ (M_{\odot}) | $a_1 \sin i$ (R_{\odot}) | d (pc) | T_{eff} (K) | $\log g$ |
|----------|------------|-------|---------------------------|---------------------------------|-------------|-------------------------|----------|
| HD 14633 | 15.4082 | 0.700 | 0.0040 | 4.13 | 2040 | 35100 | 3.95 |
| HD 15137 | 30.35 | 0.48 | 0.004 | 6.7 | 2420 | 29700 | 3.50 |

TABLE 2
SUMMARY OF GREEN BANK TELESCOPE OBSERVATIONS

| Star | Receiver | MJD – 2450000 | Orbital Phase | Exposure time (s) | S_{lim} (μJy) | L_{lim} (mJy kpc^2) |
|----------|----------|------------------|------------------|----------------------|--|--|
| HD 14633 | S-band | 3909.4194 | 0.381 | 6300 | 15 | 0.062 |
| | 820 MHz | 3909.5085 | 0.387 | 6300 | 100 | 0.42 |
| HD 15137 | S-band | 3897.4847 | 0.482 | 6300 | 15 | 0.088 |
| | 820 MHz | 3897.5753 | 0.485 | 6300 | 65 | 0.38 |

TABLE 3
TERMINAL VELOCITY MEASUREMENTS

| Star | N V $\lambda 1238.821$ V_{∞} (km s^{-1}) | Si IV $\lambda 1393.76$ V_{∞} (km s^{-1}) | C IV $\lambda 1548.202$ V_{∞} (km s^{-1}) | Adopted V_{∞} (km s^{-1}) |
|----------|---|--|--|--|
| HD 14633 | 1677 | ... | ... | 1677 ± 10 |
| HD 15137 | 1660 | 1710 | 1690 | 1690 ± 25 |

TABLE 4
OBSERVED X-RAY FLUX LIMITS

| | HD 14633 | HD 15137 |
|---|------------------------|------------------------|
| Value of $n\text{H}$ (cm^{-2}) | 6.76×10^{20} | 2.22×10^{21} |
| Upper limit of count rate (cts s^{-1}) | 0.00587 | 0.0129 |
| Energy band of <i>ROSAT</i> /PSPC observation (keV) | 0.24 – 2.0 | 0.1 – 2.4 |
| Assumed Γ | 2.0 | 2.0 |
| Unabsorbed F_X , 0.5 – 10 keV band ($\text{erg cm}^{-2} \text{s}^{-1}$) | 1.60×10^{-13} | 5.62×10^{-13} |
| Assumed Γ | 1.6 | 1.6 |
| Unabsorbed F_X , 0.5 – 10 keV band ($\text{erg cm}^{-2} \text{s}^{-1}$) | 2.39×10^{-13} | 7.85×10^{-13} |